A Pilot Study of Photon Counting CT Spectral Analysis Following Pancreatic Adenocarcinoma Resection to Differentiate Local Recurrence From Postsurgical Fibrosis

Samantha Platt, MD, Bhavik Bansal, MBBS,† Barun Bagga, MBBS,MD,‡ Thomas O'Donnell, Phd,§ and Bari Dane, MD**

Objective: To assess photon counting CT (PCCT) spectral parameters in the differentiation of locally recurrent pancreatic adenocarcinoma (PDAC) from benign postsurgical fibrosis after PDAC surgical resection.

Methods: Twenty-two patients [12 male, mean ± SD: age 71 (8) y] who underwent pancreas protocol PCCT following surgery for PDAC were retrospectively identified. Local recurrence required tissue histopathology or enlarging FDG-avid soft tissue. Non-recurrence required soft-tissue reduction with stable or decreased CA 19-9. Two blinded radiologists independently drew regions of interest within the surgical bed soft tissue to determine iodine density (I), I normalized to aortic enhancement (I%), fat fraction, and extracellular volume (ECV), which were compared using the Mann-Whitney *U* test. *A* $P < 0.05$ indicated statistical significance. The intraclass correlation coefficient was used to assess inter-reader reliability. ROC analysis was performed using mean measurements.

Results: On pancreatic parenchymal phase imaging, median [IQR] postcontrast attenuation for patients with nonrecurrence (n = 10) and recurrence (n = 11) was 32.3 (16.4 to 42.9 HU) and 57.0 (50.2 to 65.5 HU)($P = 0.001$); enhancement was 23.7 (10.2 to 26.0 HU) and 40.0 (34.4 to 44.5 HU) ($P = 0.001$); I was 0.6 (0.5 to 0.90 mg/mL) and 1.8 (1.5 to 2.0 mg/mL) ($P < 0.001$); I% was 8.3 (6.3% to 11.1%) and 34.3 (29.8% to 40.9%) ($P < 0.001$); and ECV was 5.8 (4.4 to 6.9 mL) and 23.0 (18.0 to 25.8 mL) ($P < 0.001$), respectively. To differentiate nonrecurrent from recurrent soft tissue, a post-contrast 45.7 HU threshold had 100% sensitivity and 80% specificity [AUC = 0.92 (0.80-1.00)]; enhancement of 31.9 HU had 81.8% sensitivity and 100% specificity [AUC = 0.98 (0.93-1.00)]; 14.0 mL ECV had 100% sensitivity and 100% specificity [AUC = 1.00 (1.00-1.00)]; 1.27 mg/mL I had 90.9% sensitivity and 100% specificity [AUC = 0.99 (0.98-1.00)]; and 20.3% I% had 100% sensitivity and 100% specificity (AUC = 1.00). Inter-reader agreement was near-perfect (ICCs 0.86 to 0.96).

Conclusions: PCCT spectral parameters demonstrated excellent diagnostic performance in differentiating locally recurrent PDAC from postsurgical fibrosis on pancreatic parenchymal phase imaging.

Key Words: photon counting CT, pancreatic adenocarcinoma, recurrent neoplasm, iodine density, extracellular volume

(*J Comput Assist Tomogr* 2026;00:00–00)

Pancreatic ductal adenocarcinoma (PDAC) is the sixth most common cause of cancer death globally, with 5-year survival rates estimated at 11%.[1–3] Most patients present with either locally advanced disease (30% to 35%) or metastatic disease (50%) at diagnosis, typically precluding resection.[3,4] In patients with localized PDAC, surgery, such as pancreaticoduodenectomy or distal pancreatectomy, is the only potentially curative treatment and improves survival.[3–6]

After surgical resection, soft-tissue attenuation within the resection bed on CT can present a diagnostic challenge. While this may represent benign post-treatment fibrosis, locoregional recurrence can have a similar morphologic appearance, as this also often presents as ill-defined, perivascular, or infiltrative soft tissue. Radiologists often rely on size change between CT examinations to assess for either stability or size reduction, which favors benign scarring, or interval growth, which is highly concerning for recurrent disease.[7–9] Particularly in patients who have undergone a pancreaticoduodenectomy, tissue sampling of surgical bed findings may not be technically feasible.[10] PET-CT may be of limited value if the primary PDAC was not highly FDG-avid, and because post-surgical fibrosis is often FDG-avid as well.[9,11] Mischaracterization can lead to false reassurances or delay in appropriate treatment planning, which increases patient and provider anxiety and may lead to an unnecessary treatment change or termination.

Multienergy or spectral CT, including both dual-energy CT (DECT) and photon-counting CT (PCCT), enables advanced spectral processing, such as iodine density determination.[12–18] Iodine density functions as a surrogate marker of tissue perfusion because it reflects the iodine content within a voxel, whereas traditional Hounsfield Units (HU) incorporate the intrinsic tissue attenuation.[19] Importantly, iodine density is only obtainable from multi-energy CT. Prior DECT studies demonstrated that material decompensation aids in the diagnosis of PDAC due to increased soft tissue contrast[20] and PDAC iodine density correlates with perfusion parameters in dynamic contrast-enhanced CT.[21,22] DECT iodine density also correlates with histopathologic PDAC response and can be used to differentiate local recurrence from postsurgical changes.[16,23]

Received for publication July 6, 2026; accepted September 19, 2026.

From the *From the Department of Radiology, NYU Langone Health, New York; †Department of Internal Medicine, Division of Cardiology, University of Texas Southwestern Medical Center, Dallas, TX; ‡Department of Radiology, NYU Langone Health, Mineola, NY; and §Siemens Healthineers, Malvern, PA.

Bari Dane is on the Olympus IBD advisory board and has received a speaker honorarium, research support, and travel support from Siemens Healthineers. Thomas O'Donnell is a Siemens Healthineers employee. The other authors have no conflicts of interest to report. The remaining authors have no conflict of interest or financial disclosures to report.

Correspondence to: Samantha Platt, MD, Department of Radiology, NYU Langone Health, 660 1st Avenue, New York, NY 10016 (e-mail: samantha.platt@nyulangone.org).

Copyright © 2026 Wolters Kluwer Health, LLC. All rights reserved.

DOI: 10.1097/RCT.0000000000001935

Copyright © 2026 Wolters Kluwer Health, LLC. Unauthorized reproduction of this article is prohibited.

In conjunction with hematocrit, CT-derived iodine analysis can also be used to calculate extracellular volume (ECV), a marker of the cellular environment that can be used to subtype malignancies, estimate fibrotic burden, and predict tumor aggressiveness and response.[24–29] Previous studies have shown that ECV is increased in pancreatic fibrosis and malignancies.[25,30] In addition, elevated ECV in PDAC has been shown to correlate with improved overall and progression-free survival.[31,32] ECV has been shown to predict tumor response to neoadjuvant therapy, and, following therapy, lower ECVs were observed in patients with a favorable response.[33,34] The hematocrit used in the calculation should be as close to the exam date as possible; however, a recent study found no significant difference between using a hematocrit measured within 1 week of the exam and a same-day measurement.[35] In addition to iodine and ECV analysis, fat fraction can be obtained on spectral CT and may correlate with the risk of developing PDAC.[36] However, in a postoperative PDAC PCCT study, fat fraction was unable to distinguish local recurrence from nonrecurrent tissue.[37]

PCCT is a relatively new form of spectral CT that can directly convert X-rays into electrical signals, bypassing a visual light intermediate. The energy of each incident photon is measured by the semiconductor detector; thus, spectral information is always available, and, with it, iodine density for clinically relevant protocols.[38,39] PCCT iodine density has been validated in many other systems and disease processes, including in Crohn's disease as a marker of active inflammation,[14] to differentiate renal masses from benign cysts,[40] and in the assessment of pathologic treatment response in rectal cancer.[41] Specifically regarding PDAC, PCCT's inherently improved iodine contrast-to-noise ratio allows for improved primary tumor conspicuity[42] and substantial inter-reader agreement for PDAC vascular involvement and metastasis identification, even with 40% radiation exposure adjustment, compared with moderate agreement at conventional energy-integrating detector CT.[43] At PCCT, a pilot study found that preoperative PDAC iodine density had an excellent correlation with histopathologic treatment response, with higher iodine density in PDAC neoadjuvant therapy responders,[44] suggesting iodine density as a noninvasive biomarker. Another early study showed that PCCT iodine density and normalized iodine density are higher in local recurrence than in postoperative fibrosis.[37]

Spectral parameters have shown promise for this differentiation at DECT; however, there is limited data supporting their utility at PCCT. In addition, to our knowledge, there are no studies assessing PCCT-determined ECV in the diagnosis of PDAC recurrence. Therefore, the purpose of our study was to retrospectively assess PCCT spectral parameters, including iodine density, ECV, and fat fraction, to differentiate post-surgical fibrosis from recurrent neoplasm and aid noninvasive diagnosis.

METHODS

Patients

This study received institutional review board approval and was Health Insurance Portability and Accountability Act compliant. The requirement for written informed consent was waived.

Adult outpatients (≥18 y) who underwent a clinical pancreatic protocol abdominal PCCT (Naeotom Alpha, Siemens Healthineers, Forchheim, Germany) between May 2022 and November 2025, with surgically resected and pathology-proven PDAC, were identified by retrospective departmental Picture Archiving and Communication search (PACS, Visage, San Diego, CA). Exclusions included patients without PDAC, without soft tissue at the surgical bed, or with PCCTs that did not contain the special spectral imaging dataset required for retrospective spectral postprocessing (SPP) on thin-client software. One postoperative PCCT was included per patient (with a minimum interval of 30 d), and the closest CT to the surgery date was selected, as indeterminate surgical bed soft tissue can be difficult to interpret without comparison exams. If the patient had more recent examinations, subsequent abdominal CTs were also reviewed by the radiologists for evidence of growing tissue suspicious for local recurrence.

Reference Standard

The reference standard utilized a composite of histopathology, multidisciplinary pancreatic cancer tumor board discussion, CA 19-9 values, as well as soft tissue growth or regression on subsequent imaging based on imaging review by a fellowship-trained abdominal radiologist with 8 years' experience and 6 years of multidisciplinary pancreas conference coverage, and PET assessment. Local recurrence was defined as growing soft tissue on serial imaging examinations (>20% increase in size from postoperative index examination)[45] that was pathology-proven or PET FDG-avid (uptake greater than background liver parenchyma).[46] The multidisciplinary tumor board determination was required and utilized for all patients. Cancer Antigen 19-9 (CA 19-9) values were noted as well. Nonrecurrence was defined as the absence of soft-tissue growth with a stable or decreased CA 19-9 level.[47,48] One patient without soft-tissue growth and a positive CA 19-9 level was reviewed by the radiologist and an oncologist and deemed to have no local recurrence, with elevated CA 19-9 levels secondary to distant metastatic disease. The surgical bed findings in this patient demonstrated 96 days of stability on imaging.

The electronic medical record was reviewed for surgical histopathology from biopsy or re-resection, use of neoadjuvant therapy regimen, and CA 19-9 level, preoperatively, closest to surgery, and postoperatively, closest to the PCCT date. A hematocrit level closest to the CT date was used to determine ECV, calculated as $(1 - hematocrit) * \left(\frac{lesion\ iodine\ concentration}{aorta\ iodine\ concentration}\right)$.

Photon-Counting CT Imaging Technique

PCCT examinations were performed on a first-generation dual-source PCCT (NAEOTOM Alpha, Siemens Healthineers, Forchheim, Germany) with 2 cadmium telluride photon-counting detector arrays and acquired in multienergy mode (QuantumPlus) with 120 kVp tube voltage, 144 × 0.4 mm collimation, automatic tube current modulation (CARE Dose4D), and Care keV IQ level 145. Assessment of surgical bed soft tissue was performed on images in the axial plane acquired during the pancreatic parenchymal and portal venous phases of contrast enhancement after 40 seconds or 70 seconds following the injection of intravenous contrast, respectively. 4 mm axial, 3 mm coronal, and 3 mm sagittal images at 70 keV, 4 mm axial 55 keV pancreatic parenchymal phase, as well as 0.8 mm axial SPP images allowing for retrospective spectral analysis were reconstructed and sent to PACS as well as an independent thin-client server (SyngoVia, VA50, Siemens

Copyright © 2026 Wolters Kluwer Health, LLC. All rights reserved.
Copyright © 2026 Wolters Kluwer Health, LLC. Unauthorized reproduction of this article is prohibited.

Healthineers, Forchheim, Germany). Pancreatic protocol CT was requested by the referrer in all cases, as many of these patients underwent vascular reconstructions.

Computed tomography dose index volume ($CTDI_{vol}$), dose-length product (DLP), and size-specific dose estimate (SSDE) were recorded from PACS. Time elapsed between PCCT and surgery, as well as the most recent abdominal imaging, was recorded.

Photon-Counting CT Quantitative Spectral Analysis

PCCT examinations were deidentified and sent to the thin-client server for spectral analysis. Surgical bed soft tissue was identified through careful review of the native imaging in PACS by a fellowship-trained abdominal radiologist with 8 years of post-fellowship experience. Two independent radiologists, including the abdominal radiologist and a third-year radiology resident, who were blinded to imaging interpretation, clinical parameters, outcome, and the other radiologist's measurements, placed region-of-interest (ROI) measurements independently using the thin-client server on surgical bed soft tissue on 70 keV images. In separate sessions, each radiologist placed a freehand ROI as large as possible within the surgical bed soft tissue (minimum of 20 HU), excluding normal pancreatic parenchyma, adjacent organs, surrounding fat, and neighboring vasculature. Iodine density was normalized to the aorta at the level of the celiac artery, excluding calcified and noncalcified abdominal aortic plaque. The ROI size, mean attenuation (HU), and standard deviation on both the contrast-enhanced and virtual noncontrast (VNC) images, lesion enhancement (HU) calculated as the difference between VNC and postcontrast attenuation, iodine density (mg/mL), normalized iodine density as a percentage of aortic enhancement (%), and fat fraction (%) were recorded. Aorta iodine density at the level of the celiac artery was also recorded to calculate ECV, as described above. Results reported are the mean of the 2 readers.

Statistical Analysis

Continuous variables were summarized as median (IQR), and group comparisons were performed using the Mann-Whitney *U* test (nonparametric; small sample sizes). Categorical variables were compared with the Fisher exact test. Imaging data were analyzed separately for the pancreatic and portal venous phases for each reader, and as a combined estimate. Inter-reader agreement was assessed by the intraclass correlation coefficient (two-way mixed, absolute agreement model). ROC curves were constructed using the DeLong method, and the Youden index was used to identify optimal thresholds. Statistical significance was set at $P < 0.05$. All analyses were performed in (R Studio version 4.2.2; Posit PBC, Boston, MA).

RESULTS

Patients

A PACS search for PCCT with pathology-proven PDAC within 6 months yielded 161 unique patients. One hundred thirty-nine patients were excluded as follows: preoperative study (n = 73), no surgery (n = 50), no follow-up imaging to ensure an appropriate diagnosis (n = 7), no PDAC (n = 5), and no SPP images to allow for retrospective spectral postprocessing (n = 4). This resulted in a final cohort of 22 patients [12 men and 10 women, mean ± SD age: 71 (8) y] (Table 1; Fig. 1).

17/22 patients (77%) underwent a Whipple procedure, and 5/22 (23%) had a distal pancreatectomy. The most common tumor stage among patients was T2 (11/22, 50%). Postoperative CA 19-9 levels were significantly lower in the nonrecurrent group (33.2 vs. 232.3 U/mL, $P = 0.04$). Local recurrence had growing soft tissue on serial imaging examinations that was pathology-proven (n = 4) or PET FDG-avid (n = 4). CA 19-9 values were available for 18 (81.8%) of patients. One patient in the recurrent group underwent radiation therapy. Age, sex, tumor stage, neoadjuvant or adjuvant therapy regimen, surgery type, preoperative resectability (resectable, borderline, or locally advanced), preoperative CA 19-9 levels, and hematocrit did not differ between patients with and without local recurrence (all $P > 0.05$) (Table 1).

Imaging

The median (IQR) time between PCCT and surgery was 143 (56 to 325) days and was significantly shorter in the nonrecurrence group, 57 (41) days, compared with 324 (167) days in the recurrent group ($P < 0.001$) (Table 1). The median (IQR) days between PCCT and the most recent abdominal imaging were not significantly different between the groups, 486 (282 to 730) days in the benign fibrosis versus 319 (150 to 428) days in the recurrence group ($P = 0.18$). The median (IQR) CTDvol was 24.9 (16.6 to 31.7) mGy, DLP was 573.2 (393.7 to 839.5) mGycm, and SSDE was 35.7 (25.0 to 42.9) mGy (Table 1).

Photon-Counting CT Pancreatic Parenchymal Phase Spectral Analysis

Pancreatic parenchymal phase imaging was available for 10 patients in the nonrecurrent group and 11 patients in the recurrence group.

The median (IQR) for nonrecurrence and recurrence for postcontrast attenuation was 32.3 (16.4 to 42.9 HU) and 57.0 (50.2 to 65.5 HU) [$P = 0.001$, ICC = 0.96 (95% CI: 0.90-0.98)]; lesional enhancement was 23.7 (10.2 to 26.0 HU) and 40.0 (34.4 to 44.5 HU) ($P = 0.001$), respectively; iodine density was 0.62 (0.48 to 0.89 mg/mL) and 1.8 (1.5 to 2.0 mg/mL), respectively [$P < 0.001$, ICC = 0.96 (95% CI: 0.90-0.98)]; normalized iodine density was 8.3(6.3% to 11.1%) and 34.3 (29.8% to 40.9%), respectively [$P < 0.001$, ICC = 0.96 (95% CI: 0.91-0.99)]; and ECV was 5.8 (4.4 to 6.9 mL) and 23.0 (18.0 to 25.8 mL) ($P < 0.001$). There was no significant difference in the soft tissue fat fraction between the groups ($P = 0.31$) (Table 2; Figs. 2, 3). Inter-reader agreement was near-perfect with ICCs ranging from 0.86 to 0.96 (all $P > 0.05$, Table 2).

For differentiating nonrecurrence from recurrence, a minimum postcontrast attenuation of 45.7 HU had 100% sensitivity and 80% specificity (AUC = 0.92, 95% CI: 0.80-1.00); lesion enhancement of 31.9 HU had 81.8% sensitivity and 100% specificity [AUC = 0.98 (0.93-1.00)]; 14.0 mL ECV had 100% sensitivity and 100% specificity [AUC = 1.00 (1.00-1.00)]; a 1.27 mg/mL iodine density had 90.9% sensitivity and 100% specificity [AUC = 0.99 (0.98-1.00)]; and 20.3% normalized iodine density had 100% sensitivity and 100% specificity [AUC = 1.00 (1.00-1.00)] (Table 3; Figs. 2, 3).

Photon-Counting CT Spectral Portal Venous Phase Subanalysis

Portal venous phase imaging was available for 7 patients without recurrence and for 5 patients with

Copyright © 2026 Wolters Kluwer Health, LLC. All rights reserved.

Copyright © 2026 Wolters Kluwer Health, LLC. Unauthorized reproduction of this article is prohibited.

TABLE 1. Patient Demographics

Characteristic	Overall N = 22, n (%)	Benign Fibrosis N = 10, n (%)	Recurrence N = 12, n (%)	*P*
Sex				0.70†
Male	12 (55)	6 (60)	6 (50)	
Female	10 (45)	4 (40)	6 (50)	
Age (y)*	70 (66-75)	69 (65-75)	70 (68-72)	0.70‡
$CTDI_{vol}$ (mGy)*	24.9 (16.6, 31.7)	30.1 (23.6, 35.4)	19.1 (14.0, 28.1)	0.56‡
DLP (mGy-cm)*	573.2 (393.7, 839.5)	693.6 (595.2, 1031.7)	395.5 (352.2, 622.5)	**0.03**‡
SSDE (mGy)*	35.7 (25.0, 42.9)	40.4 (34.9, 45.7)	26.8 (21.4, 42.2)	0.12‡
Time between PCCT and surgery (d)*	142.5 (56.3, 325.3)	56.5 (47.3, 128.3)	323.5 (159.3, 492.3)	**0.001**‡
Surgery				0.80†
Whipple	17 (77)	7 (70)	10 (83)	
Distal pancreatectomy splenectomy	5 (23)	3 (30)	2 (17)	
Resection status				**0.011**†
R0	15 (68)	10 (100)	5 (42)	
R1	7 (32)	0 (0)	7 (58)	
Classification of resectability				0.9†
Resectable	8 (36)	4 (40)	4 (33)	
Borderline	11 (50)	5 (50)	6 (50)	
Locally advanced	3 (14)	1 (10)	2 (17)	
Stage				0.90†
T1N0M0	4 (18)	2 (20)	2 (17)	
T2N0M0	5 (23)	2 (20)	3 (25)	
T2N1M0	3 (13)	1 (10)	2 (17)	
T2N2M0	3 (13)	2 (20)	1 (8)	
T3N0M0	3 (13)	1 (10)	2 (17)	
T3N1M0	2 (10)	1 (10)	1 (8)	
T4N0M0	2 (10)	1 (10)	1 (8)	
Neoadjuvant therapy				0.70†
FOLFOX	1 (5)	1 (10)	0	
FOLFIRINOX	8 (36)	5 (50)	3 (25)	
Modified FOLFIRINOX	2 (9)	0	2 (16)	
Gemcitabine/Abraxane	3 (14)	1 (10)	2 (16)	
None	8 (36)	3 (30)	5 (43)	
Adjuvant therapy				0.2†
FOLFIRINOX	8 (35)	3 (30)	5 (43)	
Modified FOLFIRINOX	3 (13)	3 (30)	0	
Gemcitabine/Abraxane	5 (22)	2 (20)	3 (25)	
Gemcitabine/Cisplatin	1 (5)	1 (10)	0	
Gemcitabine	2 (10)	0	2 (16)	
5-FU	1 (5)	0	1 (8)	
FOLFIRI	1 (5)	0	1 (8)	
None	1 (5)	1 (10)	0	
CA 19-9 (U/mL)*				
Preoperative level	116.0 (22.1, 217.8)	128.0 (51.7, 173.0)	48.3 (21.3, 820.4)	0.9‡
Postoperative level	90.8 (33.0, 428.6)	33.2 (17.2, 54.1)	232.3 (93.9, 522.8)	**0.04**‡
Hematocrit	32.8 (30.4, 36.8)	34.1 (32.8, 37.6)	31.6 (29.6, 35.0)	0.2†

Statistically significant comparisons are listed in boldface.
*Reported as median (IQR).
†Fisher exact test.
‡Wilcoxon rank sum test
$CTDI_{vol}$ indicates volume computed tomography dose index; DLP, dose length product; FOLFIRINOX, Leucovorin calcium (folinic acid), fluorouracil, irinotecan hydrochloride, and oxaliplatin; FOLFOX, Folinic acid, fluorouracil, and oxaliplatin; SSDE, size-specific dose estimate.

recurrence, as SPP images were unavailable in PACS for the remaining patients.

The median (IQR) for nonrecurrence and recurrence for postcontrast attenuation was 42.2 (21.0 to 52.0 HU) and 83.3 (74.9 to 86.4 HU), respectively [$P = 0.009$, ICC = 0.96 (95% CI: 0.87-0.99)]; lesion enhancement was 27.6 (7.5 to 34.1 HU) and 47.7 (38.7 to 50.1 HU), respectively ($P = 0.02$); iodine density was 0.95 (0.4 to 1.3 mg/mL) and 1.8 (1.3 to 2.0 mg/mL), respectively [$P = 0.03$, ICC = 0.96 (95% CI: 0.88-0.99)]; normalized iodine density was 17.5 (12.7% to 28.0%) and 37.4 (33.6% to 44.2%), respectively [$P = 0.006$, ICC = 0.94 (95% CI: 0.82-0.98)]; and ECV was 10.2 (7.2 to 17.5 mL) and 24.7 (22.0 to 28.0 mL), respectively ($P = 0.009$). There was no significant difference in fat fraction between the groups ($P = 0.10$) (Table 4).

For differentiating between nonrecurrence and recurrence, a 19.4 mL ECV had 100% sensitivity and 85.7% specificity [AUC = 0.97 (0.89-1.00); a 1.10 mg/mL iodine density had 100% sensitivity and 71.4% specificity AUC = 0.89 (0.69-1.00); and a 33.1% normalized iodine density had 100% sensitivity and 100% specificity AUC = 1.00 (1.00-1.00)].

DISCUSSION

Surgical bed soft tissue on postsurgical CT can present a diagnostic challenge. In our study of 22 patients who

Copyright © 2026 Wolters Kluwer Health, LLC. All rights reserved.
Copyright © 2026 Wolters Kluwer Health, LLC. Unauthorized reproduction of this article is prohibited.

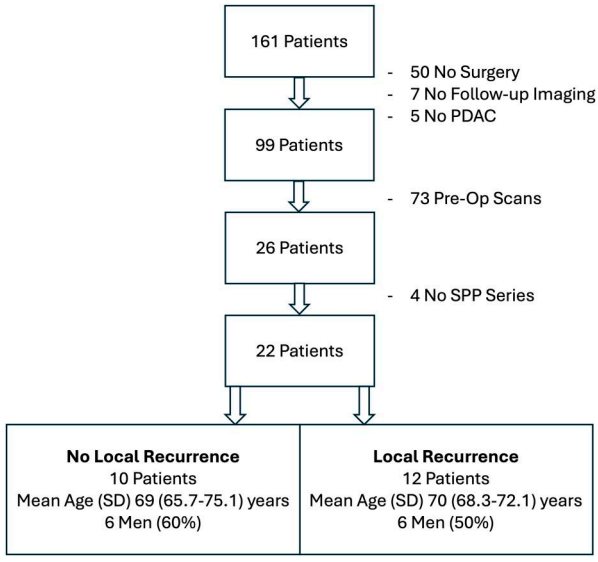


FIGURE 1. Patient demographics.

underwent PCCT after PDAC resection, ECV and iodine density analysis had perfect diagnostic performance for differentiating local recurrence from post-surgical fibrosis (100% sensitivity and specificity). Thresholds of 14.0 mL for ECV, 1.27 mg/mL for iodine density, and 20.3% for normalized iodine density at pancreatic parenchymal phase PCCT differentiated benign postsurgical change from locally recurrent neoplasm, which can be difficult to distinguish based on conventional imaging appearance. This distinction can have critical implications for treatment planning and prognosis.

PCCT iodine density analysis in our study outperformed typical post-contrast HU measurements and enhancement in differentiating recurrence from postsurgical fibrosis. Both postcontrast HU and enhancement were significantly higher in recurrent compared with non-recurrent soft tissue ($P \leq 0.001$). These had lower sensitivity and specificities (100% and 80%, 81.8% and 100%, respectively) relative to iodine density (90.9% and 100%), normalized iodine density, and ECV (both 100% sensitivity and specificity). Our study is consistent with DECT literature reporting that iodine density can distinguish postoperative recurrence from fibrosis.[23] In addition, prior PCCT studies have shown that increased iodine concentration can be seen with malignant lesions and is superior to HU contrast enhancement.[37,40] Alagic et al[37] demonstrated that PCCT iodine density and normalized iodine density are increased in PDAC local recurrence relative to postoperative fibrosis, which is concordant with our results. Comparatively, our pancreatic parenchymal phase iodine density and normalized iodine density thresholds demonstrated improved sensitivity and specificity compared with their model, which showed 94% sensitivity and 84% specificity.[37] In addition, that study did not investigate postcontrast attenuation or ECV, both of which, in our study, were significantly elevated in recurrent tissue, with ECV showing perfect diagnostic performance. It is valuable that postcontrast attenuation and lesion enhancement were significantly higher in recurrence compared with fibrosis, as many radiologists interpret monoenergetic exams without leveraging spectral analysis. Although iodine density and normalized iodine density were superior and may be used for

TABLE 2. Quantitative Analysis Comparing Benign Fibrosis and Recurrence on Pancreatic Parenchymal Phase Imaging Through Mann-Whitney *U* Test Reported as Median (IQR)

Characteristic	Benign Fibrosis N = 10	Recurrence N = 11	*P*	Median ICC (95% CI)
VNC (HU)	21.8 (−3.6 to 26.6)	17.9 (12.5-25.0)	> 0.99	0.90 (0.77-0.96)
Reader 1	20.6 (−2.1 to 25.6)	18.10 (13.5-27.6)		
Reader 2	21.6 (−0.3 to 30.1)	17.1 (9.6-22.1)		
Postcontrast attenuation (HU)	32.3 (16.4-42.9)	57.0 (50.2-65.6)	**0.001**	0.96 (0.90-0.98)
Reader 1	0.4 (0.3-1.0)	0.3 (0.3-0.5)		
Reader 2	33.0 (16.3-44.5)	52.0 (47.6-65.8)		
Lesion enhancement (HU)	23.7 (10.20-26.0)	39.7 (34.4-44.5)	**< 0.001**	
Reader 1	23.2 (11.8-27.6)	39.4 (34.9-46.0)		
Reader 2	21.0 (8.7-28.8)	37.8 (33.8-43.9)		
ROI area (cm^2)	0.4 (0.3-0.7)	0.4 (0.2-0.5)	0.75	0.83 (0.62-0.93)
Reader 1	0.4 (0.3-1.0)	0.3 (0.3-0.5)		
Reader 2	0.3 (0.2-0.6)	0.4 (0.2-0.6)		
Fat fraction	20.3 (16.1-35.9)	28.7 (21.1-34.8)	0.31	
Reader 1	20.6 (15.4-35.1)	29.2 (19.5-33.3)		
Reader 2	19.9 (16.6-34.5)	30.0 (23.5-34.3)		
Extracellular volume (mL)	5.8 (4.4-6.9)	23.0 (18.0-25.8)	**< 0.001**	
Reader 1	5.9 (4.1-7.1)	23.0 (16.8-25.7)		
Reader 2	5.4 (4.2-7.4)	23.0 (17.8-25.2)		
Iodine density (mg/mL)	0.6 (0.5-0.9)	1.8 (1.5-2.0)	**< 0.001**	0.96 (0.90-0.98)
Reader 1	0.6 (0.5-0.8)	1.8 (1.5-2.2)		
Reader 2	0.7 (0.5-0.9)	1.7 (1.5-2.0)		
Normalized iodine density	8.3 (6.3-11.1)	34.25 (29.8-40.9)	**< 0.001**	0.96 (0.91-0.99)
Reader 1	8.5 (5.8-10.9)	34.3 (29.7-39.5)		
Reader 2	8.9 (6.3-10.9)	36.1 (30.9-42.3)		

Statistically significant comparisons are listed in boldface.
Collective and individual data are reported in the initial row for each listed characteristic.

Copyright © 2026 Wolters Kluwer Health, LLC. All rights reserved.

Copyright © 2026 Wolters Kluwer Health, LLC. Unauthorized reproduction of this article is prohibited.

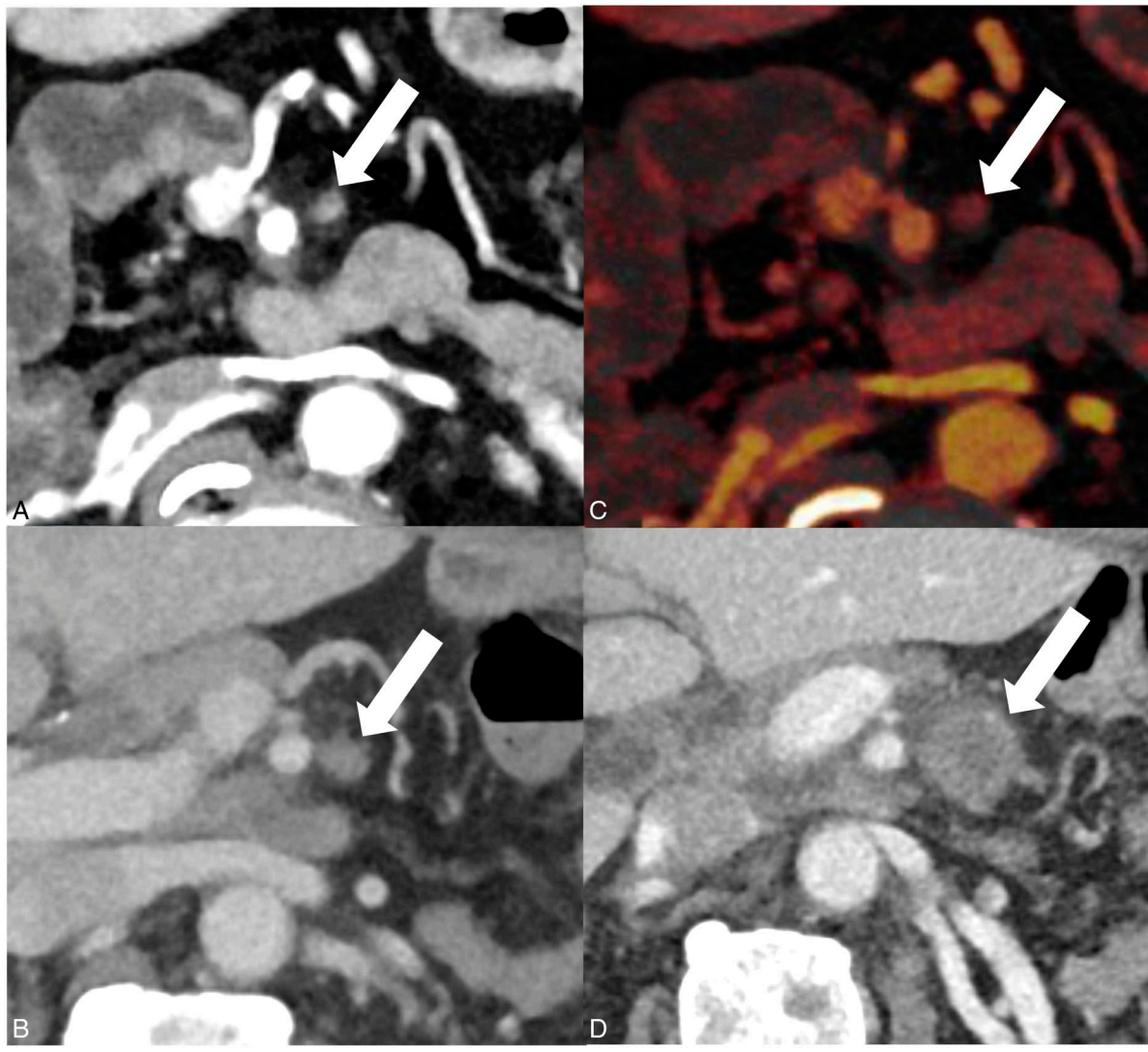


FIGURE 2. A 69-year-old man after Whipple for PDAC (441 d postoperative) with a soft tissue nodule (arrows) in the surgical bed on axial pancreatic phase (A) and portal venous phase PCCT (B). Iodine map in the pancreatic phase demonstrates iodine density 1.55 mg/mL, 28.0% normalized to aortic enhancement, 25.2% fat fraction, and ECV 19.3 mL (C). Follow-up portal-venous-phase abdominal CT (613 d postoperative) demonstrates a marked increase in nodule size (D). Imaging findings are consistent with local recurrence. Iodine analysis and ECV values are above our reported thresholds. The multidisciplinary pancreas tumor board agreed with the interpretation.

challenging interpretations, it is reassuring that HU alone can distinguish local recurrence from fibrosis on PCCT. Importantly, iodine analysis and ECV are independent of the virtual monoenergetic level utilized for routine interpretation, whereas HU will vary.[49] As most readers routinely view virtual monoenergetic reconstructions in clinical practice, a robust quantitative parameter unaffected by energy level is imperative.[49]

In our PCCT study, ECV was significantly higher in recurrent lesions than in nonrecurrent lesions ($P < 0.001$), with perfect sensitivity and specificity. In DECT, ECV has been shown to be elevated in pancreatic cancer,[30] and elevated PDAC ECV correlates with improved overall and progression-free survival.[31,32,50] Malignancies manipulate the tumor microenvironment and often expand the extracellular matrix through fibrosis and stromal activation, which increases ECV.[51,52] As fibrosis is a key feature of PDAC, we hypothesized that ECV expansion associated with fibrosis was greater in recurrent lesions than in postsurgical fibrosis. Hematocrit levels are key to the ECV calculation, and in our study, we used the lab value closest to the exam date, even if many were not from the same day. It is reassuring and consistent with the current literature that recent, but not necessarily same-day, hematocrit levels can be used to calculate ECV.[35] Given that both ECV and normalized iodine density thresholds had perfect sensitivity and specificity, we recommend using normalized iodine density over ECV for patients with significant hematocrit abnormalities, as normalized iodine density is independent of hematocrit. Overall, our data are consistent with the current literature indicating that ECV is elevated in PDAC, but to our knowledge, no studies have evaluated the

Copyright © 2026 Wolters Kluwer Health, LLC. All rights reserved.
Copyright © 2026 Wolters Kluwer Health, LLC. Unauthorized reproduction of this article is prohibited.

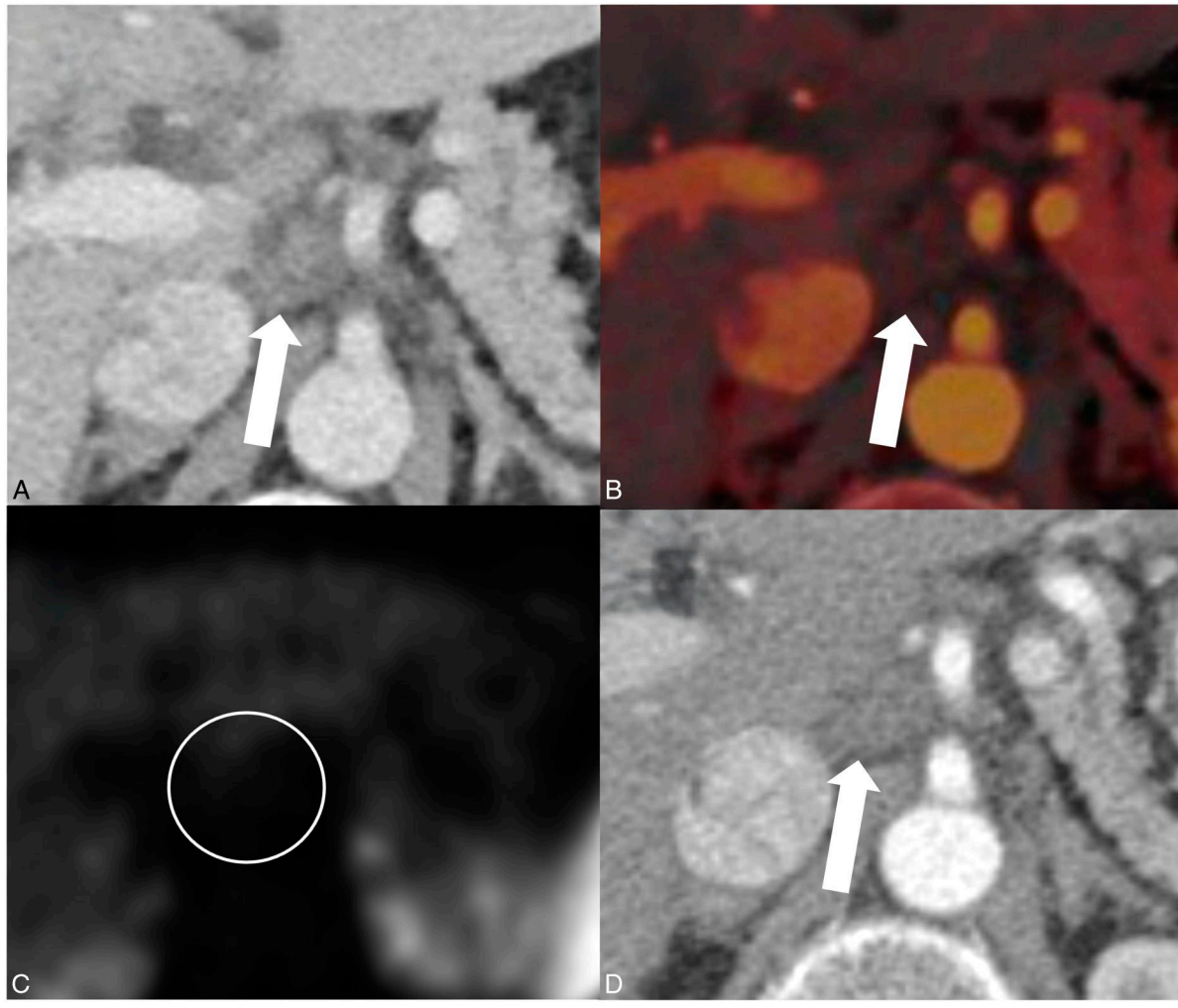


FIGURE 3. A 53-year-old woman after Whipple for PDAC (120 d postoperative) with retroperitoneal soft tissue (arrows) on pancreatic parenchymal phase PCCT (A). Iodine concentration 1.1 mg/mL on iodine map (B), 11.9% normalized to aortic enhancement, 19.5% fat fraction, and 7.8 mL ECV. FDG-18 PET CT (144 d postoperative) demonstrates no lesion uptake (circle) (C). Surveillance CT (400 d postoperative) demonstrates unchanged soft tissue (D). Findings are consistent with benign, postoperative fibrosis and no local recurrence. Iodine analysis and ECV values are below our reported threshold. The multidisciplinary tumor board agreed with the interpretation.

relationship between ECV and PDAC on PCCT or, more specifically, whether it can be used to distinguish locally recurrent PDAC from benign postsurgical fibrosis.

The final PCCT spectral parameter assessed was fat fraction. While it was hypothesized that postsurgical fibrosis would have more interspersed fat than recurrent neoplasm and consequently a different fat fraction, our study found no significant difference in fat fraction. At baseline, the pancreas contains a relatively high fat content compared with other solid organs, which can be replaced in both oncologic and fibrotic processes.[30] Our findings are concordant with prior literature that on PCCT, fat fraction

TABLE 3. ROC Analysis of Postcontrast Attenuation, Enhancement, Fat Fraction, Extracellular Volume, Iodine Density, and Normalized Iodine Density to Differentiate Benign Fibrosis From Recurrence on Pancreatic Parenchymal Phase Imaging

Characteristic	Optimal Threshold, (%)	Sensitivity, (%)	Specificity, (%)	Area under ROC Curve (95% CI)
Postcontrast attenuation	45.8 HU	100	80	0.92 (0.80-1.00)
Lesion enhancement	31.9 HU	81.8	100	0.98 (0.93-1.00)
Fat fraction	20.0 %	90.9	50	0.64 (0.36-0.91)
ECV	14.0 mL	100	100	1.00 (1.00-1.00)
Iodine density	1.27 mg/mL	90.9	100	0.99 (0.98-1.00)
Normalized iodine density	20.3 %	100	100	1.00 (1.00-1.00)

Copyright © 2026 Wolters Kluwer Health, LLC. All rights reserved.

Copyright © 2026 Wolters Kluwer Health, LLC. Unauthorized reproduction of this article is prohibited.

TABLE 4. Quantitative Analysis Comparing Benign Fibrosis and Recurrence on Portal Venous Phase Imaging Through Mann- Whitney *U* Test Reported as Median (IQR)

Characteristic	Benign Fibrosis N = 7	Recurrence N = 5	*P*	Median ICC (95% CI)
VNC (HU)	18.0 (2.6-25.9)	33.2 (30.6-36.2)	0.10	0.87 (0.61-0.96)
Reader 1	16.7 (6.5-27.7)	38.4 (31.0-41.0)		
Reader 2	15.4 (2.9-26.1)	30.2 (29.9-34.0)		
Postcontrast attenuation (HU)	42.2 (21.0-52.0)	83.3 (74.9-86.4)	**0.009**	0.96 (0.87-0.99)
Reader 1	35.4 (25.7-53.4)	85.8 (71.4-92.2)		
Reader 2	48.5 (17.8-50.8)	80.6 (78.3-80.8)		
Lesion enhancement (HU)	27.6 (7.5-34.1)	47.6 (38.7-50.1)	**0.02**	
Reader 1	29.1 (8.1-34.7)	44.8 (33.0-49.3)		
Reader 2	26.1 (7.8-33.5)	46.0 (44.3-55.4)		
ROI Area (cm^2)	0.3 (0.3-0.6)	0.2 (0.2-0.6)	0.62	0.59 (0.06-0.86)
Reader 1	0.3 (0.2-0.4)	0.2 (0.2-0.3)		
Reader 2	0.4 (0.2-0.8)	0.2 (0.2-0.9)		
Fat fraction (%)	25.9 (16.9-35.3)	15.8 (11.4-16.3)	0.10	
Reader 1	24.3 (17.2-31.9)	14.3 (9.3-17.1)		
Reader 2	27.4 (18.7-36.0)	17.2 (15.5-17.7)		
Extracellular volume (mL)	10.2 (7.2-17.5)	24.7 (22.0-28.0)	**0.009**	
Reader 1	10.7 (4.9-16.6)	23.7 (20.5-26.8)		
Reader 2	13.0 (7.9-18.2)	25.7 (24.4-29.2)		
Iodine Density (mg/mL)	1.0 (0.4-1.3)	1.8 (1.3-2.0)	**0.03**	0.96 (0.88-0.99)
Reader 1	1.0 (0.3-1.3)	1.6 (1.2-2.0)		
Reader 2	0.9 (0.5-1.3)	2.0 (1.3-2.0)		
Normalized Iodine Density (%)	17.5 (12.7-28.0)	37.4 (33.6-44.2)	**0.006**	0.94 (0.82-0.98)
Reader 1	18.6 (9.1-28.9)	34.5 (33.5-43.0)		
Reader 2	23.2 (12.8-26.8)	41.2 (35.8-45.4)		

Statistically significant comparisons are listed in boldface.
Collective and individual data are reported in the initial row for each listed characteristic.

cannot definitively differentiate locally recurrent PDAC from postsurgical change.[37]

One patient demonstrated difficult-to-interpret findings on pancreatic parenchymal phase imaging, with an iodine density of 1.15 mg/mL, which was below the 1.27 mg/mL threshold. However, their normalized iodine density (34.3%) and ECV (24.0 mL) were appropriately above the thresholds (20.3% and 14.0 mL), as was the mean post-contrast enhancement (54.0 HU). This lesion enlarged on subsequent imaging and was deemed a local recurrence based on tumor board consensus and rising CA 19-9 levels. Reassuringly, this lesion could have been appropriately diagnosed using conventional post-contrast attenuation at 70 keV, ECV, or normalized iodine density.

In our subanalysis of portal venous phase imaging, which is typically performed in the surveillance of patients who underwent surgery for PDAC, postcontrast attenuation at 70 keV, iodine density, normalized iodine density, and ECV were all significantly higher in the recurrent group; however, these parameters had decreased sensitivities and specificities relative to their corresponding thresholds calculated from the pancreatic parenchymal phase. To reduce image acquisition time in PACS, fewer patients had available SPP portal venous-phase images than pancreatic parenchymal-phase images, thereby reducing our sample size and likely affecting diagnostic performance. After surgery, the portal venous phase is typically the only imaging phase obtained to assess for recurrence; however, pancreatic parenchymal phase images were obtained in our study at the referrer's request in the setting of vascular reconstructions. Although our sample size for portal venous imaging was small, our findings were generally similar to those from pancreatic parenchymal phase imaging.

Limitations of our study include that this is a single-center, retrospective study by a single vendor PCCT with a small sample size; however, there was only 1 clinically available PCCT at the time of this study. Selection bias due to the large number of excluded patients is inevitable, and larger future studies are needed. In addition, not all lesions had surgical pathology confirming whether the postoperative soft tissue was benign fibrosis or recurrence; however, this reflects clinical practice, in which these patients often do not undergo tissue sampling. We ensured substantial imaging follow-up, particularly for nonrecurrent patients [median (IQR) 486 (282 to 730 d)], and that all patients had a multidisciplinary tumor board discussion to serve as a reference standard. In our recurrent group, significantly more patients had R^1 resection status, which may also have contributed to the increased risk of recurrence compared with the nonrecurrent group. In addition, while it is recommended that hematocrit be measured within 1 week of CT to accurately determine ECV, in our study, it was often measured later. However, ECV remained a valuable tool in our study.

In conclusion, PCCT pancreatic parenchymal phase ECV and iodine density analyses are highly sensitive and specific for differentiating benign fibrosis from recurrent tumor in the PDAC surgical bed. This powerful tool has the potential to help radiologists in their diagnosis and appropriately guide the oncologic team in their decision-making.

REFERENCES

1. Huang J, Lok V, Ngai CH, et al. Worldwide burden of, risk factors for, and trends in pancreatic cancer. *Gastroenterology*. 2021;3:744–754.
2. Siegel RL, Miller KD, Fuchs HE, et al. Cancer statistics, 2022. *CA Cancer J Clin*. 2022;1:7–33.

Copyright © 2026 Wolters Kluwer Health, LLC. All rights reserved.

Copyright © 2026 Wolters Kluwer Health, LLC. Unauthorized reproduction of this article is prohibited.

3. de Jesus VHF, Riechelmann RP. Current treatment of potentially resectable pancreatic ductal adenocarcinoma: a medical oncologist's perspective. *Cancer Control*. 2023;30: 10732748231173212.
4. Park W, Chawla A, O'Reilly EM. Pancreatic cancer: a review. *JAMA*. 2021;9:851–862.
5. Katz MH, Taylor TH, Al-Refaie WB, et al. Adenosquamous versus adenocarcinoma of the pancreas: a population-based outcomes analysis. *J Gastrointest Surg*. 2011;1:165–174.
6. Springfeld C, Ferrone CR, Katz MHG, et al. Neoadjuvant therapy for pancreatic cancer. *Nat Rev Clin Oncol*. 2023;5: 318–337.
7. Budigi B, Oliphant M, Itri J. Pancreatic adenocarcinoma: diagnostic errors, contributing factors and solutions. *Acad Radiol*. 2022;7:967–976.
8. Adair A, Oniscu A, Wigmore SJ. Postsurgical pancreatitis masquerading as recurrent neuroendocrine cancer. *J Surg Case Rep*. 2010;4:1.
9. Chu LC, Wang ZJ, Kambadakone A, et al. Postoperative surveillance of pancreatic ductal adenocarcinoma (PDAC) recurrence: practice pattern on standardized imaging and reporting from the Society of Abdominal Radiology disease focus panel on PDAC. *Abdom Radiol (NY)*. 2023;1:318–339.
10. Pua U, Quek LH. Modified retroperitoneal access for percutaneous intervention after pancreaticoduodenectomy. *Korean J Radiol*. 2013;3:446–450.
11. Yeh R, Dercle L, Garg I, et al. The Role of 18F-FDG PET/CT and PET/MRI in Pancreatic Ductal Adenocarcinoma. *Abdom Radiol (NY)*. 2018;2:415–434.
12. Dane B, Kernizan A, O'Donnell T, et al. Crohn's disease active inflammation assessment with iodine density from dual-energy CT enterography: comparison with endoscopy and conventional interpretation. *Abdom Radiol (NY)*. 2022;10:3406–3413.
13. Dane B, Li X, Goldberg JD, et al. Crohn's disease phenotype analysis with iodine density from dual-energy CT enterography. *Abdominal Radiology*. 2023;7:2219–2227.
14. Dane B, Qian K, Soni R, et al. Crohn's disease inflammation severity assessment with iodine density from photon counting CT enterography: comparison with endoscopic histopathology. *Abdom Radiol (NY)*. 2024;1:271–278.
15. Dane B, Sarkar S, Nazarian M, et al. Crohn disease active inflammation assessment with iodine density from dual-energy CT enterography: comparison with histopathologic analysis. *Radiology*. 2021;1:144–151.
16. Ohira S, Ikawa T, Kanayama N, et al. Dual-energy computed tomography-based iodine concentration as a predictor of histopathological response to preoperative chemoradiotherapy for pancreatic cancer. *J Radiat Res*. 2023;6:940–947.
17. Gordic S, Puippe GD, Krauss B, et al. Correlation between dual-energy and perfusion CT in patients with hepatocellular carcinoma. *Radiology*. 2016;1:78–87.
18. Hellbach K, Sterzik A, Sommer W, et al. Dual energy CT allows for improved characterization of response to antiangiogenic treatment in patients with metastatic renal cell cancer. *Eur Radiol*. 2017;6:2532–2537.
19. McCollough CH, Leng S, Yu L, et al. Dual- and multi-energy CT: principles, technical approaches, and clinical applications. *Radiology*. 2015;3:637–653.
20. Noda Y, Hattori M, Kawai N, et al. Novel silicon-based material decomposition images in diagnosis of pancreatic ductal adenocarcinoma: comparison with iodine-based and 50-keV virtual monoenergetic images. *Jpn J Radiol*. 2026;1: 106–115.
21. Bao J, Liu A, Zhao C, et al. Correlation between dual-energy computed tomography single scan and computed tomography perfusion for pancreatic cancer patients: initial experience. *J Comput Assist Tomogr*. 2019;4:599–604.
22. Stiller W, Skornitzke S, Fritz F, et al. Correlation of quantitative dual-energy computed tomography iodine maps and abdominal computed tomography perfusion measurements: are single-acquisition dual-energy computed tomography iodine maps more than a reduced-dose surrogate of conventional computed tomography perfusion? *Invest Radiol*. 2015;10:703–708.
23. Mathy RM, Fritz F, Mayer P, et al. Iodine concentration and tissue attenuation in dual-energy contrast-enhanced CT as a potential quantitative parameter in early detection of local pancreatic carcinoma recurrence after surgical resection. *Eur J Radiol*. 2021;143:109944.
24. Liu J, Zhang X, Lv R, et al. Predictive value of extracellular volume fraction determined using enhanced computed tomography for pathological grading of clear cell renal cell carcinoma: a preliminary study. *Cancer Imaging*. 2025;1:49.
25. Martuszewski A, Paluszkiewicz P, Poręba R, et al. Clinical significance of extracellular volume of myocardium (ECV) assessed by computed tomography: a systematic review and meta-analysis. *J Clin Med*. 2025;6:2066.
26. Fu X, Guo Y, Zhang K, et al. Prognostic impact of extracellular volume fraction derived from equilibrium contrast-enhanced CT in HCC patients receiving immune checkpoint inhibitors. *Sci Rep*. 2025;1:13643.
27. Iwaya H, Fukukura Y, Hashimoto S, et al. Prognostic significance of extracellular volume fraction with equilibrium contrast-enhanced computed tomography for pancreatic neuroendocrine neoplasms. *Pancreatology*. 2021;4: 779–786.
28. Li J, Zou L, Ma H, et al. Interpretable machine learning based on CT-derived extracellular volume fraction to predict pathological grading of hepatocellular carcinoma. *Abdom Radiol (NY)*. 2024;10:3383–3396.
29. Bandula S, Punwani S, Rosenberg WM, et al. Equilibrium contrast-enhanced CT imaging to evaluate hepatic fibrosis: initial validation by comparison with histopathologic sampling. *Radiology*. 2015;1:136–143.
30. Fukui H, Onishi H, Nakamoto A, et al. Pancreatic fibrosis by extracellular volume fraction using Contrast-enhanced computed tomography and relationship with pancreatic cancer. *Eur J Radiol*. 2022;156:110522.
31. Ming S, Zhang W, Wang M, et al. Contrast-enhanced CT-derived extracellular volume fraction predicts survival in postoperative pancreatic cancer patients. *Eur J Radiol*. 2025; 191:112273.
32. Fukukura Y, Kumagae Y, Higashi R, et al. Estimation of extracellular volume fraction with routine multiphasic pancreatic computed tomography to predict the survival of patients with stage IV pancreatic ductal adenocarcinoma. *Pancreas*. 2019;10:1360–1366.
33. Fujita N, Ushijima Y, Itoyama M, et al. Extracellular volume fraction determined by dual-layer spectral detector CT: possible role in predicting the efficacy of preoperative neoadjuvant chemotherapy in pancreatic ductal adenocarcinoma. *Eur J Radiol*. 2023;162:110756.
34. Noid G, Godfrey G, Hall W, et al. Predicting treatment response from extracellular volume fraction for chemoradiation therapy of pancreatic cancer. *Int J Radiat Oncol Biol Phys*. 2023;3:803–808.
35. Han L, Zhang T, Liu X, et al. Extended validity of hematocrit for dual-energy CT extracellular volume calculation in cirrhosis: a 7-day window enhances clinical utility. *J Comput Assist Tomogr*. 2026;50:520–525.
36. Korn RL, Burkett A, Geschwind J, et al. Can imaging using radiomics and fat fraction analysis detect early tissue changes on historical CT scans in the regions of the pancreas gland that subsequently develop adenocarcinoma? *Diagnostics (Basel)*. 2023;13:941.
37. Alagic Z, Duran CV, Svensson-Marcial A, et al. Contrast-enhanced photon-counting detector CT for discriminating local recurrence from postoperative changes after resection of pancreatic ductal adenocarcinoma. *Eur Radiol Exp*. 2025;1:26.
38. Flohr T, Petersilka M, Henning A, et al. Photon-counting CT review. *Phys Med*. 2020;79:126–136.
39. Rajendran K, Petersilka M, Henning A, et al. First clinical photon-counting detector CT system: technical evaluation. *Radiology*. 2022;1:130–138.

Copyright © 2026 Wolters Kluwer Health, LLC. All rights reserved.

Copyright © 2026 Wolters Kluwer Health, LLC. Unauthorized reproduction of this article is prohibited.

40. Platt S, Bansal B, Bagga B, et al. Renal lesion assessment at portal venous phase photon counting computed tomography: iodine concentration and attenuation analysis. *J Comput Assist Tomogr*. 2026;1:28–37.
41. Surov A, Diallo-Danebrock R, Radi A, et al. Photon counting computed tomography in rectal cancer: associations between iodine concentration, histopathology, and treatment response: a pilot study. *Acad Radiol*. 2024;9:3620–3626.
42. Decker JA, Becker J, Härting M, et al. Optimal conspicuity of pancreatic ductal adenocarcinoma in virtual monochromatic imaging reconstructions on a photon-counting detector CT: comparison to conventional MDCT. *Abdom Radiol (NY)*. 2024;1:103–116.
43. Kim J, Mabud T, Huang C, et al. Inter-reader agreement of pancreatic adenocarcinoma resectability assessment with photon-counting versus energy-integrating detector CT. *Abdom Radiol (NY)*. 2024;9:3149–3157.
44. Shou A, Bagga B, Hajdu C, et al. A pilot study to assess pancreatic adenocarcinoma treatment response with iodine density from photon counting CT. *J Comput Assist Tomogr*. 2026;50:13–19.
45. Ruchalski K, Dewan R, Sai V, et al. Imaging response assessment for oncology: an algorithmic approach. *Eur J Radiol Open*. 2022;9:100426.
46. Huang S, Chong H, Sun X, et al. The Value of (18)F-FDG PET/CT in diagnosing pancreatic lesions: comparison with CA19-9, enhanced CT, or enhanced MR. *Front Med (Lausanne)*. 2021;8:668697.
47. Ballehaninna UK, Chamberlain RS. Serum CA 19-9 as a biomarker for pancreatic cancer: a comprehensive review. *Indian J Surg Oncol*. 2011;2:88–100.
48. Azizian A, Rühlmann F, Krause T, et al. CA19-9 for detecting recurrence of pancreatic cancer. *Sci Rep*. 2020;1:1332.
49. Dane B, Ananthakrishnan L, Marin D, et al. Adult abdominal photon-counting CT protocols: a multi-institutional consensus of the Society of Abdominal Radiology Photon-Counting Detector CT Emerging Technology Commission. *AJR Am J Roentgenol*. 2025;6:e2533625.
50. Xiong J, Lu Y, Liu H, et al. Extracellular volume derived from equilibrium CT for the prediction of survival outcomes in patients with pancreatic ductal adenocarcinoma. *Technol Cancer Res Treat*. 2025;24:15330338251336032.
51. Liu J-Y, Wang Q, Lu Y-T, et al. MRI-derived extracellular volume fraction as a prognostic biomarker for early recurrence after R0 resection of pancreatic ductal adenocarcinoma. *Eur J Radiol Open*. 2025;15:100711.
52. Lafaro KJ, Melstrom LG. The paradoxical web of pancreatic cancer tumor microenvironment. *Am J Pathol*. 2019;1:44–57.

Copyright © 2026 Wolters Kluwer Health, LLC. All rights reserved.
Copyright © 2026 Wolters Kluwer Health, LLC. Unauthorized reproduction of this article is prohibited.